文章编号：1001-9014(XXXX)XX-0001-07

DOI:10.11972/j.issn.1001-9014.XXXX.XX.001

Characteristics Analysis of 1.06um Long-cavity Diode Lasers Based on Asymmetric Waveguide Structures

ZHAO Ren-Ze, GAO Xin, FU Ding-Yang, ZHANG Yue, SU Peng, BO Bao-Xue*

(National Key Lab of High-Power Semiconductor Lasers, Changchun University of Science and Technology, Changchun 130022, China)

Abstract: 在长腔边发射二极管激光器中,纵向空间烧孔(LSHB),双光子吸收(TPA)和自由载流子吸收(FCA)是影响高注入电流下输出功率线性增长的关键因素。本文针对1.06um波长长腔半导体激光器,通过将TPA和FCA损耗与一维速率方程相结合,提出一种简化数值分析模型。系统分析了LSHB,TPA和FCA对输出特性的影响,并提出可以通过调整前腔面反射率和量子阱(QW)在波导中的位置来提高前腔面输出功率。

Key words: semiconductor lasers, longitudinal spatial hole burning, free carrier absorption, two-photon absorption

PACS:

基于非对称波导结构的1.06um长腔半导体激光器特性分析

赵仁泽, 高 欣, 伏丁阳, 张 悦, 苏 鹏, 薄报学*

(长春理工大学高功率半导体激光国家重点实验室,吉林长春 130022)

关 键 词:半导体激光器;纵向空间烧孔;自由载流子吸收;双光子吸收

中图分类号:TN248.4　　**文献标识码**:A

In long-cavity edge-emitting diode lasers, longitudinal spatial hole burning (LSHB), two-photon absorption (TPA) and free carrier absorption (FCA) are among the key factors affecting the linear increase in output power at high injection currents. In this paper, a simplified numerical analysis model is proposed for 1.06um wavelength long-cavity diode lasers by combining TPA and FCA losses with one-dimensional (1D) rate equations. The effects of LSHB, TPA and FCA on the output characteristics are systematically analyzed, and it is proposed that the front facet reflectivity and the position of the quantum well (QW) in the waveguide can be adjusted to improve the front facet output power.

1 Introduction

1.06 um diode lasers are widely used in LIDAR, laser fuzes, laser ranging, optoelectronic countermeasures, laser blinding and target identification. Usually, high power edge-emitting diode lasers are coated with high and low reflectivity films on both cavity facets to improve slope efficiency. On the other hand, in order to reduce the thermal resistance, long cavity is adopted for high power diode lasers, which mitigates the temperature rise in the active region[1]. However, the above design in practical devices can aggravate the non-uniform distribution of carrier density along the cavity length, a phenomenon known as longitudinal spatial hole burning (LSHB)[2-3]. The LSHB can lead to an increase in threshold current and a decrease in slope efficiency[4].

Two-photon absorption (TPA) and free carrier absorption (FCA) are considered as the main mechanisms limiting the output power[5-6]. High power diode lasers tend to have a large waveguide layer[7], which is typically a few microns thick, contain a thin active region consisting of one or more quantum well (QW) layers, and the thickness of n-side waveguide is greater than the p-side waveguide (the absorption cross section of holes is much larger than that of electrons, so the waveguide loss of p-side tend to be more severe, and a low waveguide loss by FCA can be achieved by reducing the p-side waveguide thickness).

Usually, there are two types of TPA loss: (i) the di-

Foundation items: Supported by National Key R&D Project (No. 2017YFB0405100), National Natural Science Foundation of China (No. 61774024/61964007) and Jilin province science and technology development plan (No. 20190302007GX).

Biography: Zhao Renze (1999-), male, Nanyang China, postgraduate. Research area involves high power semiconductor laser. E-mail: 1310495184@qq.com.

* **Corresponding author**: E-mail: bbx@cust.edu.cn

rect light absorption loss, namely direct TPA loss. (ii) TPA will also produce free carriers, which can further attenuate the light field by free carrier absorption, namely indirect TPA loss[8]. TPA loss of diode lasers with symmetric waveguide has been studied with experimentally measured parameters[5,9]. In this paper, waveguide losses including TPA loss in asymmetric waveguide structures are analysed to optimize the output characteristics of long-cavity diode lasers, while FCA loss due to current injection is also considered.

2 Waveguide structures of lasers

The one-dimension waveguide structure of a typical high power diode laser is shown in Fig. 1. h is the thickness of the waveguide layer, the position of the QW in the waveguide layer is noted as p_x and $\Psi^2(x)$ is the normalized mode field intensity distribution, $\int_{-\infty}^{+\infty}\Psi^2(x)dx = 1$. Since the QW thickness (10nm) is much smaller than the waveguide layer in Fig. 1, the optical mode field of the device is mainly determined by the waveguide and confinement layers, which can be expressed approximately by the mode field distribution in a three-layer slab waveguide[10]:

$$\Psi(x) = \begin{cases} \frac{1}{C_0}\cos(kx - \varphi), & 0 < x < h \\ \frac{1}{C_0}cos\varphi \exp(\gamma_n x), & x < 0 \\ \frac{1}{C_0}\cos(kh - \varphi)\exp(-\gamma_p(x - h)), & x > h \end{cases} \quad (1)$$

Wherek = $\frac{2\pi}{\lambda}\sqrt{n_{wg}^2 - n_o^2}$ is the transverse wave vector, $\gamma_n = \frac{2\pi}{\lambda}\sqrt{n_o^2 - n_n^2}$ and $\gamma_p = \frac{2\pi}{\lambda}\sqrt{n_o^2 - n_p^2}$ are the field decrements in the n and p confinement layers, respectively. $\varphi = \arctan(\frac{\gamma_n}{k})$, and $C_0 = \sqrt{(h + \frac{1}{\gamma_n} + \frac{1}{\gamma_p})/2}$. The effective refractive index of the fundamental mode n_o can be obtained from the transcendental equation $kh = \arctan\left(\frac{\gamma_n}{k}\right) + \arctan(\frac{\gamma_p}{k})$.

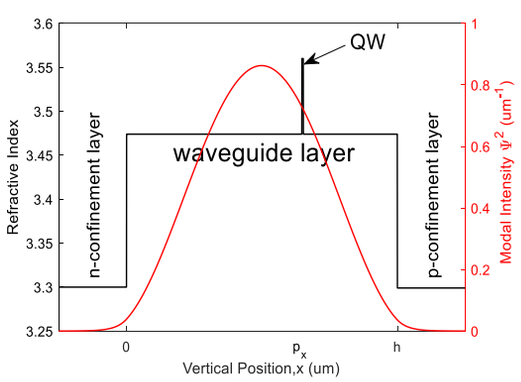

Fig. 1 The fundamental mode intensity and index profiles of the waveguide structure
图1 波导的折射率和基模强度分布

3 Theoretical model

In this paper, losses related to direct and indirect TPA, FCA due to current injection in the waveguide, and material loss are considered for performance simulation of long-cavity diode lasers with the effect of LSHB. The direct TPA loss can be expressed as[11]

$$\alpha_{TPA}^{direct} = \frac{P(z)}{w}\int_{-\infty}^{\infty}\beta(x)\psi^4(x)dx, \quad (2)$$

$\beta(x)$ is the TPA coefficient for different materials in the waveguide structure. As shown in Fig. 1, the TPA loss in the confinement layer can be neglected because of the weak mode field in the confinement layer, and previous studies have found that the contribution of QW to TPA is negligible compared to the waveguide regions[5], so the total TPA loss is contributed by the waveguide layer(GaAs). The direct TPA loss can be further simplified as

$$\alpha_{TPA}^{direct} = \frac{\beta_{wg}P(z)}{w}\int_0^h\psi^4(x)dx, \quad (3)$$

P(z) is the mode power along the cavity, w is the ridge waveguide width and β_{wg} is the TPA coefficient for waveguide layer. In order to deal with the direct TPA loss with the 1D rate equations, the direct TPA loss can be expressed as a function of the photon density along the cavity. P(z) is given versus photon density $N_p(z)$ by the following:

$$P(z) = \frac{wd}{\Gamma}v_g\frac{h_1 c}{\lambda}N_p(z), \quad (4)$$

where h_1 is Planck's constant, v_g is the group velocity of light, λ is wavelength, c is the speed of light in vacuum, and d is the quantum well thickness. The confinement factor is expressed by the following equation:

$$\Gamma = \frac{\int_{p_x - \frac{d}{2}}^{p_x + \frac{d}{2}}\psi^2(x)dx}{\int_{-\infty}^{+\infty}\Psi^2(x)dx}. \quad (5)$$

Substituting (4) into (3), we obtain that

$$\alpha_{\mathrm{TPA}}^{direct} = \frac{\beta_{wg} dv_g h_1 c}{\Gamma\lambda}\int_0^h \psi^4(x)\,dx N_p(z) = \beta_{TPA}^{direct} N_p(z), \quad (6)$$

where $\beta_{TPA}^{direct} = \frac{\beta_{wg} dv_g h_1 c}{\Gamma\lambda}\int_0^h \psi^4(x)\,dx$, is the direct TPA coefficient. Since the waveguide layer is undoped intentionly, there is quasi-neutrality within the waveguide layer, i. e. the electrons and holes have the same density, and then the carrier transport can be described by the ambipolar diffusion equation:

$$D_a \frac{\partial^2 N}{\partial^2 x} + G(x,z) - R\left(N(x,z)\right) = 0, \quad (7)$$

where $\mathrm{D_a} = \frac{2\mathrm{D_e D_h}}{\mathrm{D_e} + \mathrm{D_h}}$, $\mathrm{D_e}$ and $\mathrm{D_h}$ are the electron and hole diffusion coefficients in the waveguide layer, respectively. The indirect TPA loss is caused by the absorption of light by TPA-generated carriers, and the TPA-generated carrier density distribution can be obtained, based on the TPA generation term[11]:

$$\mathrm{G(x,z)} = \frac{\beta_{\mathrm{wg}}\lambda}{h_1 c}\left(\frac{P(z)}{w}\right)^2 \psi^4(x). \quad (8)$$

$$= \beta_{TPA}^{indirect} N_p(z)^2,$$

where $\beta_{TPA}^{indirect} = \int_0^h (\sigma_e + \sigma_h)\gamma\psi^2(x)\,dx$, is the indirect TPA coefficient. σ_e and σ_h are the free-electron and free-hole absorption cross-sections, respectively. Neglecting the carrier recombination, the carrier density distribution in the waveguide layer can be obtained by equation (7)[6]:

$$\Delta \mathrm{N_j}(x) = \begin{cases} \frac{j}{2eD_e}\left(p_x - \frac{d}{2} - x\right) + N_b, 0 < x < p_x - \frac{d}{2} \\ \frac{j}{2eD_h}\left(x - p_x - \frac{d}{2}\right) + N_b, p_x + \frac{d}{2} < x < h \end{cases}, \quad (12)$$

where j is the current density, e is the electron charge, $\mathrm{N_b} \approx \frac{\mathrm{j}}{\mathrm{ed}}\tau$, τ is the capture time of carrier into the QW. The FCA loss in the waveguide layer can be expressed as

$$\alpha_{\mathrm{j}}^{wg} = (\sigma_e + \sigma_h)\int_0^h \Delta N_j(x)\psi^2(x)\,dx. \quad (13)$$

The FCA loss in the QW can be expressed as

$$\alpha_{\mathrm{j}}^{QW} = \Gamma(\sigma_e + \sigma_h)N(z) = \beta_j^{QW} N(z), \quad (14)$$

where $\beta_{\mathrm{j}}^{\mathrm{QW}} = \Gamma(\sigma_e + \sigma_h)$, N(z) is the carrier density in the QW. Because of LSHB, the carrier density N(z) is no longer constant, but decreases gradually from position of the rear facet to the front facet. The FCA loss in the confinement layer can be expressed as[6]

$$\alpha_{\mathrm{j}}^{cl} = (\sigma_e + \sigma_h)\left(\int_{-\infty}^0 \psi^2(x)\,dx + \int_h^{+\infty} \psi^2(x)\,dx\right) N_{cl}, \quad (15)$$

where $\mathrm{N_{cl}}$ is the doping concentration of confinement layer. The behavior of diode lasers is determined by the relationship equation between carriers and photons. It is usually assumed a uniform distribution of carrier density along the cavity length in the conventional rate equations, however this is not the case in high power diode lasers. Considering the inhomogeneity and the effects of the losses above, the 1D rate equations for diode lasers in steady state conditions are

$$\frac{\eta_i j}{ed} - R_{sp}\left(N(z)\right) - v_g g(z)\left(N_p^+(z) + N_p^-(z)\right) = 0, \quad (16)$$

$$\frac{dN_p^{\pm}(z)}{dz} = \pm\left[\Gamma \mathrm{g(z)} - \alpha_{\mathrm{i}} - \alpha_j^{wg} - \alpha_j^{cl} - \beta_j^{QW} N(z) - \beta_{TPA}^{direct} N_p^{\pm}(z) - \beta_{TPA}^{indirect} N_p^{\pm}(z)^2\right] N_p^{\pm}(z). \quad (17)$$

The indirect TPA loss should be a function of the photon density along the cavity length, which means G (x, z) is a function of photon density. Substituting (4) into (8) gives:

$$\mathrm{G(x,z)} = \frac{\beta_{\mathrm{wg}} h_1 c}{\lambda}\left(\frac{dv_g}{\Gamma}\right)^2 \psi^4(x) N_p(z)^2. \quad (9)$$

Neglecting the carrier recombination (R=0), the distribution of the TPA-generated carrier density in the waveguide layer is obtained by combining the boundary conditions with equation (7):

$$\Delta \mathrm{N_{TPA}}(x,z) = \gamma N_p(z)^2, \quad (10)$$

where γ is a function of x and $\mathrm{p_x}$ for the n and p side waveguides. The indirect TPA loss is expressed as

$$\alpha_{\mathrm{TPA}}^{indirect} = (\sigma_e + \sigma_h)\int_0^h \Delta N_{TPA}(x,z)\psi^2(x)\,dx = \int_0^h (\sigma_e + \sigma_h)\gamma\psi^2(x)\,dx N_p^2(z)^2 \quad (11)$$

$$(12)PAjj$$

Equation(16) describes the change in carrier density due to spontaneous and stimulated recombinations, under current injection. Equation(17) describes the evolution of the photon density along the laser cavity and takes into account internal losses. α_i and η_i are the material loss and internal quantum efficiency, respectively. $N_p^+(z)$ and $N_p^-(z)$ are the photon densities for forward and backward propagation, respectively. $N_p(z) = N_p^-(z) + N_p^+(z)$ and $R_{sp}(N(z)) = AN(z) + BN(z)^2 + CN(z)^3$, is the spontaneous recombination rate. The gain coefficient can be expressed as $g(z) = g_0 \ln[N(z)/N_{tr}]$. The boundary conditions for equations(16) and (17) at the rear facet ($z = 0$) and the front facet ($z = L$) are

$$N_p^+(0) = R_{HR} N_p^-(0), \tag{18}$$

$$I_{th} = \frac{ewd}{\eta_i} \int_0^L R_{sp}(N(z))\,dz. \tag{19}$$

The front facet output power can be expressed as

$$P_{out} = (1 - R_{AR}) v_g \frac{dw}{\Gamma} \frac{h_1 c}{\lambda} N_p^+(L). \tag{20}$$

Table 1 lists the main parameters for the device simulation calculations.

Table 1 Used device parameters
表1 所用器件参数

Symbol	Parameter	Value
λ	wavelength	1.06 um
n_{wg}	refractive index of waveguide layer	3.474
n_n	refractive index of n- confinement layer	3.3
n_p	refractive index of p- confinement layer	3.3
β_{wg}	TPA coefficient for waveguide layer	2×10^{-8} cm/W
L	cavity length	5 mm
w	ridge waveguide width	100 um
d	quantum well thickness	10 nm
R_{HR}	reflectivity of rear facet	0.99
h	waveguide layer thickness	2 um
σ_e	absorption cross section of free-electron	3×10^{-18} cm^2
σ_h	absorption cross section of free-hole	1×10^{-17} cm^2
D_e	diffusion coefficient of electron	200 $cm^2\,s^{-1}$
D_h	diffusion coefficient of hole	10 $cm^2\,s^{-1}$
η_i	internal quantum efficiency	0.95
N_{cl}	doping concentration of confinement layer	1×10^{18} cm^{-3}
α_i	material loss	0.5 cm^{-1}
A	non-radiative recombination coefficient	5.88×10^8 s^{-1}
B	spontaneous emission coefficient	1×10^{-10} $cm^3\,s^{-1}$
C	auger recombination coefficient	2×10^{-30} $cm^6\,s^{-1}$
g_0	gain constant	2140 cm^{-1}
N_{tr}	transparency carrier density	1.77×10^{18} cm^{-3}
τ	capture time of carrier into the QW	150 fs

$$R_{AR} N_p^+(L) = N_p^-(L), \tag{19}$$

where R_{AR} is the front facet reflectivity, L is the cavity length. The photon and carrier density distributions along the laser cavity can be calculated by numerically solving equations(16)-(19) by the finite difference method. Threshold lasing condition can be expressed as

$$\frac{1}{L}\int_0^L \Gamma g(z)\,dz = \alpha_{i\_total} + \alpha_m, \tag{20}$$

where α_{i_total} is the total internal loss and α_m is the output loss. The threshold current can be expressed as[3]

$$\tag{21}$$

4 Results and analysis

Fig. 2 shows the $\beta_{TPA}^{indirect}$ and β_{TPA}^{direct} versus the position of QW. It can be seen that both coefficients increase gradually with p_x, because both coefficients are inversely proportional to the confinement factor, which gradually decreases as QW shifts to the p-side as shown in Fig. 4. Since the FCA and TPA losses vary with the carrier or photon density along the cavity, the average loss along the cavity is used to express the magnitude of total mode loss. Fig. 3 shows the variation of total internal loss and slope efficiency with QW positions at an injection current I=20A, R_{AR}= 0.01. It can be seen that the total internal loss decreases monotonically as QW shifts towards the p-side in the waveguide and slope efficiency has an opposite trend. The FCA loss decreases as QW shifts towards the p-side in the waveguide though the TPA loss increases with the TPA coefficients $\beta_{TPA}^{indirect}$ and β_{TPA}^{direct}. The TPA loss is too small relative to the FCA loss, to influence variation trend of total loss.

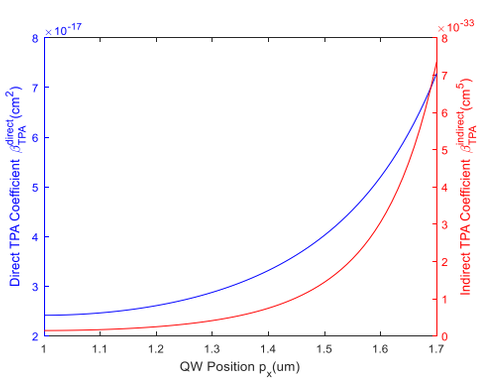

Fig. 2 The direct and indirect TPA coefficients versus
图2 直接和间接TPA系数随QW位置的变化

Fig. 4 shows the variation of the confinement factor and threshold current with the QW positions at R_{AR}= 0.01. It can be seen that the confinement factor decreases and the threshold current increases as QW shifts to-

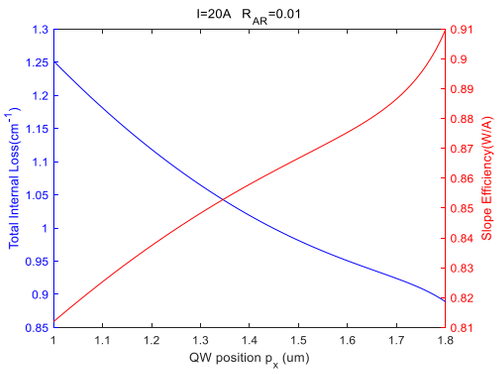

Fig. 3 Total internal loss and slope efficiency versus QW position versus QW position
图3 总内损耗和斜率效率随QW位置的变化

wards the p-side. From equations(20)(21), we can see that the threshold current is approximately an inverse function of the confinement factor. Though the total internal loss decreases as QW shifts towards the p-side, the confinement factor has a greater effect to the variation trend of threshold current.

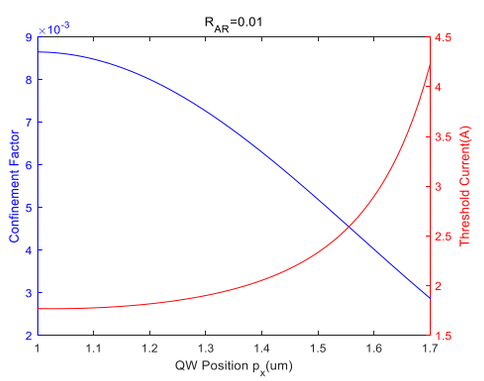

Fig. 4 Confinement factor and threshold current versus QW position
图4 限制因子和阈值电流随QW位置的变化

Since the slope efficiency and threshold current have opposite trends with QW position shifting towards the p-side, there may be a QW position that makes the front facet output power maximum. Fig. 5 shows the variation of the front facet output power with QW position for I=20A R_{AR}=0.01, and it can be seen that the maximum output is obtained at p_x=1.39um.

The front facet reflectivity plays an important role in the performance of high power diode lasers. Reducing R_{AR} improves the slope efficiency, but at the same time causes more severe LSHB. For the same injection current, the smaller R_{AR} the higher threshold current, and the optimized QW position needs to be shifted in the direction of the larger confinement factor to reduce the effect of the threshold current. Fig. 6 shows the maximum front facet output power and the corresponding QW positions vesus different front facet reflectivities at I=20A, indicating that the maximum output power can be obtained by optimization the QW position for different reflectivities

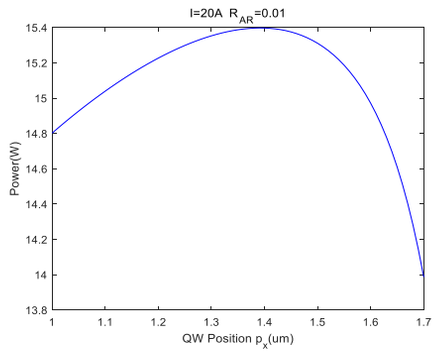

Fig. 5 Output power versus QW positions
图5 输出功率随QW位置的变化

of front cavity facets. The optimized QW positions gradually shift towards the p side as the front facet reflectivity increases. Fig. 7 shows the optimized P-I curve at I=20A.

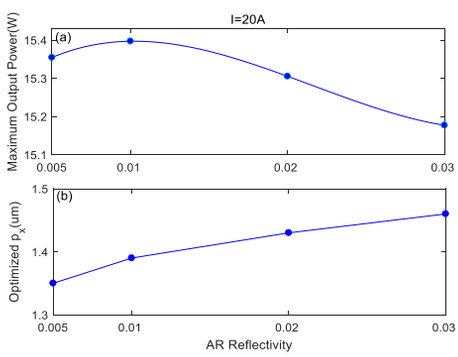

Fig. 6 (a) the maximum front facet output power and (b) optimized

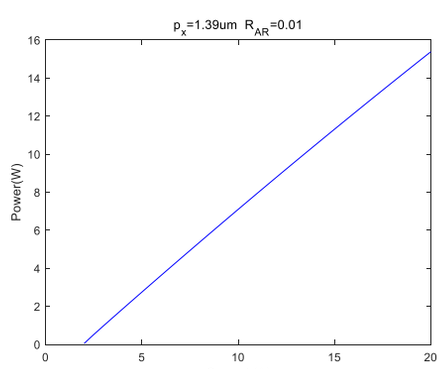

Fig. 7 P-I curve

Fig. 8 shows the optimized QW positions with injection current at R_{AR} = 0.01. It can be seen that the optimized QW position gradually shifts towards the p-side in the waveguide as the injection current increases. This is because the effect of threshold current on output power reduces as the injection current increases, so the effect of slope efficiency on output power increases relatively. The shift of the optimized QW position to the p-confinement layer tends to be slow with increasing injection cur-

rent because the smaller confinement factor the faster threshold current increases, as shown in Fig. 4.

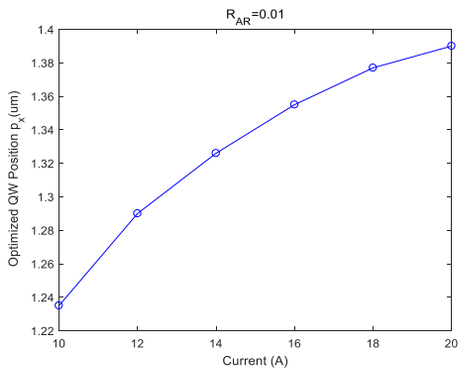

Fig. 8 The optimized QW position versus injection currents.
图8 优化后QW位置随注入电流变化

Fig. 9 gives the effect of losses on slope efficiency, threshold current and output power. It can be seen that the threshold current and slope efficiency decrease with the increase of the front facet reflectivity in Fig. 9(a). Fig. 9(b) shows that the output power increases monotonously with the decrease of the front facet reflectivity when LSHB is not considered. However, when LSHB is considered, a decrease of output power happens, because of a higher threshold current and a more significant decrease in slope efficiency at a lower front facet reflectivity as shown in Fig. 9(a). It is found that the effect of FCA loss on output power is stronger than TPA loss and LSHB becomes the most significant factor in power reduction while the front facet reflectivity is low.

5 Summary

A simplified numerical analysis model is proposed to systematically analyze the effects of LSHB, TPA and FCA on the output characteristics of 1.06 um long-cavity diode lasers. It is found that an appropriate reduction of the front facet reflectivity can increase the output power. But, too low a reflectivity will cause severe LSHB, leading to a significant reduction in the slope efficiency and a significant increase of threshold current, which in turn reduces the output power. For the same injection current, the QW position in the waveguide can be optimized for maximizing the output power. The optimized QW position moves towards the p-side in the waveguide as the front facet reflectivity or injection current increases. It is found that the effect of FCA loss on output power is stronger than TPA loss, and LSHB becomes the most significant factor affecting the output power when the front facet reflectivity is low.

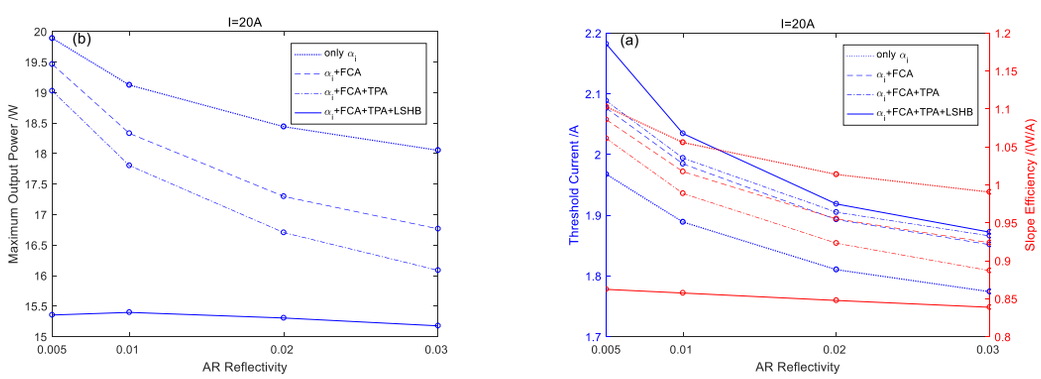

Fig.9 (a) threshold current, slope efficiency and (b) the maximum output power with the AR reflectivity.
图9 (a)阈值电流和斜率效率(b)最大输出功率随AR反射率的变化

References

[1] Chen Z G, Bao L, Bai J, *et al*.Performance limitation and mitigation of longitudinal spatial hole burning in high-power diode lasers [J]. *Proceedings of Spie the International Society for Optical Engineering*, 2012.
[2] Rinner F, Rogg J, Friedmann P, *et al*. Longitudinal carrier density measurement of high power broad area laser diodes [J]. *Applied Physics Letters*, 2002, **80**(1): 19-21.
[3] Golovin V S, Shashkin I S, Slipchenko S O, *et al*. Longitudinal spatial hole burning in high-power semiconductor lasers: numerical analysis [J]. *Quantum Electronics*, 2020, **50**(2), 147-152.
[4] Avrutin E A, Ryvkin B S. Effect of spatial hole burning on output characteristics of high power edge emitting semiconductor lasers: Auniversal analytical estimate and numerical analysis [J]. *Journal of Applied Physics*, 2019, **125**(2): 023108.1-023108.8.
[5] Dogan M, Michael C P, Zheng Y, *et al*. Two photon absorption in high power broad area laser diodes [J]. *International Society for Optics and Photonics*, 2014.
[6] Ryvkin B S, Avrutin E A. Asymmetric, nonbroadened large optical cavity waveguide structures for high-power long-wavelength semiconductor lasers [J]. *Journal of Applied Physics*, 2005, **97** (12), 123103-123103-6.
[7] Ryvkin B S, Avrutin E A. Effect of carrier loss through waveguide layer recombination on the internal quantum efficiency in large-optical-cavity laser diodes [J]. *Journal of Applied Physics*, 2005, **97** (11): 113106-113106.
[8] Juodawlkis P W, Plant J J, Donnelly J P, *et al*. Continuous-wave two-photon absorption in a watt-class semiconductor optical amplifier [J].*Optics Express*, 2008, **16**(16), 12387-96.
[9] Demir A, Peters M, Duesterberg R, *et al*. 29.5W Continuous Wave Output from 100um Wide Laser Diode [J]. *International Society for Optics and Photonics*, 2015.
[10] Kogelnik H 1975 Theory of dielectric waveguides Integrated Optics ed T Tamir (Berlin: Springer) pp 15 - 79.
[11] Avrutin E A, Ryvkin B S. Theory of direct and indirect effect of two-photon absorption on nonlinear optical losses in high power semiconductor lasers [J]. *Semiconductor Science and Technology*, 2016, **32** (1), 015004.